Journal of Medicinal Chemistry

Article

Enantioselective Nonsteroidal Aromatase Inhibitors Identified through a Multidisciplinary Medicinal Chemistry Approach

Andrea Cavalli, Alessandra Bisi, Carlo Bertucci, Carlo Rosini, Anja Paluszcak, Silvia Gobbi, Egidio Giorgio, Angela Rampa, Federica Belluti, Lorna Piazzi, Piero Valenti, Rolf W. Hartmann, and Maurizio Recanatini

J. Med. Chem., **2005**, 48 (23), 7282-7289• DOI: 10.1021/jm058042r • Publication Date (Web): 15 October 2005

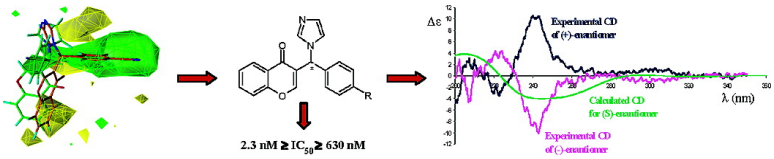

More About This Article

Additional resources and features associated with this article are available within the HTML version:

- Supporting Information
- Links to the 5 articles that cite this article, as of the time of this article download
- Access to high resolution figures
- Links to articles and content related to this article
- Copyright permission to reproduce figures and/or text from this article

View the Full Text HTML

Journal of Medicinal Chemistry is published by the American Chemical Society. 1155 Sixteenth Street N.W., Washington, DC 20036

Enantioselective Nonsteroidal Aromatase Inhibitors Identified through a Multidisciplinary Medicinal Chemistry Approach

Andrea Cavalli,[†] Alessandra Bisi,[†] Carlo Bertucci,[†] Carlo Rosini,[‡] Anja Paluszcak,[§] Silvia Gobbi,[†] Egidio Giorgio,[‡] Angela Rampa,[†] Federica Belluti,[†] Lorna Piazzi,[†] Piero Valenti,[†] Rolf W. Hartmann,[§] and Maurizio Recanatini*[,†]

Department of Pharmaceutical Sciences, University of Bologna, Via Belmeloro, 6, I-40126 Bologna, Italy, Department of Chemistry, University of Basilicata, Via N. Sauro, 85, I-85100 Potenza, Italy, and Pharmaceutical and Medicinal Chemistry, Saarland University, P. O. Box 151150, D-66041 Saarbrücken, Germany

Received July 25, 2005

To identify enantioselective nonsteroidal aromatase inhibitors, a multidisciplinary medicinal chemistry approach was pursued. First, our earlier CoMFA model [*Bioorg. Med. Chem.* **1998**, *6*, 377−388] was extended taking purposely into account previously discovered enantioselective aromatase inhibitors. The 3D QSAR model was then exploited to design chiral ligands, whose configurational assignment was obtained, after HPLC separation, by means of a combination of circular dichroism measurements and time dependent density functional calculations. Finally, the new enantiomeric inhibitors were separately tested to ascertain both their potency against the cytochrome P450 aromatase (CYP19; EC 1.14.14.1), and their selectivity relative to another enzyme of the P450 family. A satisfactory agreement between experimental and predicted data allowed us to assert that a properly built "enantioselective CoMFA model" might constitute a useful tool for addressing enantioselective ligands design.

Introduction

One of the approaches currently exploited for the treatment of postmenopausal estrogen dependent breast cancer is to reduce the estrogen's concentration in blood by means of aromatase inhibitors.[1] The aromatase enzymatic complex is formed by two proteins, namely the cytochrome P450 XIX (CYP19) and NADPH-cytochrome P450 reductase. The reaction catalyzed by the complex is the aromatization of the A ring of androgen substrates that leads to estrogen hormones. Nonsteroidal aromatase inhibitors competitively interact with the enzyme, thus displacing the natural substrate, and eventually give rise to the reduction of the estrogen's blood concentration.[2] Among different classes of aromatase inhibitors, the azole family is going to hold an increasingly prominent position, as demonstrated by azole derivatives marketed drugs.[2]

Very recently, new series of nonsteroidal aromatase inhibitors have been synthesized by different groups working in the field,[3,4] and many efforts are also being devoted to the search of dual aromatase−steroid sulfatase inhibitors,[5] which might represent a new generation of drugs targeting estrogen biosynthesis.[6]

In an earlier paper, we presented a new series of nonsteroidal aromatase inhibitors,[7] which were designed taking advantage of previously derived CoMFA models.[8,9] In that paper, we reported that CoMFA-driven suitable modifications of the (di)benzopyran-4-one nucleus allowed us to obtain potent and selective aromatase inhibitors. The most potent inhibitors of that series belonged to the azole class, and turned out to be not only almost as potent as the well-known drug fadrozole (IC_{50} = 40 and 17 nM, respectively) but also selective with respect to P450 17, another cytochrome of the P450 family involved in androgen biosynthesis.[7]

Chart 1

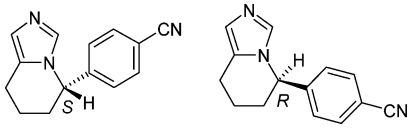

In the present paper, we report a further extension of our previous CoMFA models,[8,9] now comprising seventy structurally different nonsteroidal aromatase inhibitors. Seven of the twenty-one newly added molecules bear at least one stereogenic center and show enantioselectivity toward the aromatase enzyme. Remarkably, fadrozole itself is highly enantioselective toward P450 19,[10] as its most active enantiomer (*S*, pIC_{50} = 7.77) is two log units more potent than the least active one (*R*, pIC_{50} = 5.64) (Chart 1). Notably, since our earliest 3D QSAR studies, both enantiomers of fadrozole were taken into account in the CoMFA analyses.[8] The newly developed 3D QSAR model turned out to be statistically robust and, more important, to be able to predict different inhibitory activities for enantiomers. The obtained CoMFA model was then exploited to address the synthesis of new compounds purposely designed carrying a stereogenic center (compounds **1**−**3**, Chart 2). The compounds were synthesized, and the racemic mixtures were solved in the optically active forms by means of preparative HPLC employing chiral stationary phases. The configurational assignment of the pure enantiomers was accomplished by means of a combination of circular dichroism (CD) measurements and time dependent density functional theory (TD-DFT) calculations. Finally, the new inhibitors were biologically tested against both CYP19 and CYP17 enzymes. All of them were active at nanomolar level, selective

* Corresponding author. E-mail: maurizio.recanatini@unibo.it. Phone/fax: +39 051 2099720/34.
[†] University of Bologna.
[‡] University of Basilicata.
[§] Saarland University.

10.1021/jm058042r CCC: $30.25
Published on Web 10/15/2005

Chart 2

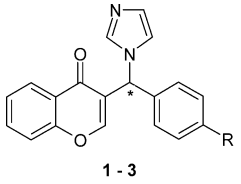

Compd.	R
1	NO_2
2	Br
3	CN

1 - 3

Scheme 1[a]

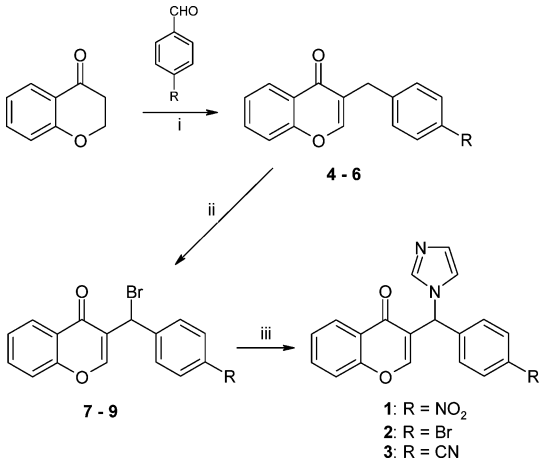

[a] Reagents: (i) piperidine, 150 °C/3 h; (ii) *N*-bromosuccinimide, CCl_4, reflux 5 h; (iii) imidazole, CH_3CN, reflux 6 h.

with respect to CYP17, and, remarkably, enantioselective toward the biological target. The fairly good agreement between the experimental and calculated pIC_{50} values for the single enantiomers showed that our work strategy was able to correctly address the design and characterization of new chiral derivatives acting enantioselectively as aromatase inhibitors. In this respect, a multidisciplinary approach to the design of enantioselective inhibitors is here presented.

Methods

Computational Chemistry. The molecular models were built by properly modifying crystallographic skeletons retrieved from the Cambridge Structural Database.[11] The models were geometrically optimized and then submitted to Monte Carlo conformational searches. The conformers were further classified by means of cluster analyses, and finally optimized at the AM1 semiempirical level. In addition, representative conformers of the new compounds were geometrically optimized within the density functional theory (DFT) framework at the B3LYP/6-31G(d) level of theory. The partial atomic charges of all 70 compounds were calculated according to the RESP procedure.[12]

The 3D QSAR analyses were carried out using the CoMFA method implemented in the SYBYL 6.9 package. The alignment of the molecules within the Cartesian space was accomplished according to the atom-by-atom procedure using both enantiomers of fadrozole as templates. For a detailed description of the alignment strategy, the reader can refer to the previously reported CoMFA models.[8,9]

Chemical Synthesis. The newly designed chiral molecules were prepared as outlined in Scheme 1. The chromanone was treated with the selected 4-substituted benzaldehyde in the presence of piperidine to afford the 3-(4-substituted)benzyl derivatives **4**−**6**, which were then brominated with *N*-bromosuccinimide with a catalytic amount of benzoyl peroxide to give intermediates **7**−**9**. Reaction with imidazole afforded the final compounds **1**−**3** reported in Chart 2.

The newly synthesized compounds **1**−**3** were obtained in optically active form by preparative HPLC resolution employing the chiral stationary phases Chiralcel OD (**1** and **3**) and Chiralcel OJ (**2**). Both stationary phases used derivatized cellulose as chiral selector.

Configurational Assignment. The absolute configuration of the separated enantiomers was determined by means of a combined approach based on experimental measurements and ab initio calculations of the chiroptical properties, i.e., optical rotation (OR) and CD.

Ab initio calculations of the OR were carried out at the TD-DFT/B3LYP/6-31G(d) level of theory and using GIAO orbitals to guarantee gauge-independency, with GAUSSIAN03 software.[13] CD calculations were carried out by using the same TD-DFT/B3LYP/6-31G(d) approach in the dipole-velocity formalism that guarantees the origin-independency. Theoretical CD spectra were obtained by overlapping Gaussian functions for each transition according to the expression

$$\Delta\epsilon(E) = \frac{1}{2.297 \times 10^{-39}} \frac{1}{\sqrt{2\pi}\sigma} \sum_{i}^{N} \Delta E_i R_i \, e^{-[(E-\Delta E_i/2\sigma)]^2}$$

In the equation, σ is the width at half-height and ΔE_i and R_i are the excitation energies (in eV) and rotary strengths (in erg esu cm/gauss) for transition i, respectively. Here, a σ value of 0.2 eV was used.[14] The conformational search was performed by means of SPARTAN02 at both the molecular mechanics (MMFF94 force field) and semiempirical (PM3) levels. The obtained geometries were then fully optimized (B3LYP/6-31G(d) level) by means of GAUSSIAN03.

Biological Assays. For the determination of biological activity, the human enzymes were used. In the case of CYP19 the tritium water method[15] and placental microsomes were employed, whereas for CYP17 the enzyme was prepared[16] from *Escherichia coli* overexpressing human CYP17.[17]

Table 1. Statistics of the PLS Analyses

component	q^2	s_{cross}	R^2	s
1	0.600	0.704	0.665	0.643
2	0.692	0.623	0.833	0.459
3	0.726	0.591	0.884	0.385
4	0.765	0.551	0.931	0.299
5	**0.791**	**0.524**	**0.958**	**0.234**
6	0.793	0.526	0.975	0.181

Results and Discussion

CoMFA Model. The present CoMFA was built by adding 21 molecules to the model developed in 1998,[9] and represents a further extension of previous ones.[8,9] In particular, the test set of the 1998 model[9] (8 molecules) along with the series of new aromatase inhibitors reported in 2001[7] (13 molecules) was added to the original training set of 49 molecules.[9] Interestingly, 7 of the newly added molecules carried at least one stereogenic center and showed enantioselectivity toward the biological target.

The statistics of the PLS analyses obtained with the 70 compounds training set are shown in Table 1. In addition, in the Supporting Information (SI), the structures of the complete set of molecules of the present CoMFA model (Figure 1SI) and the experimental and calculated pIC_{50} values of the whole set of compounds (Table 1SI) are reported. Also, a plot of the calculated vs experimental pIC_{50} is provided in Figure 2SI. Despite some poorly recalculated activity values, the extended CoMFA model is of acceptably good quality, and the overall characteristics of the previous model[9] are maintained (the interested reader is referred to the original paper for details on the interpretation of the CoMFA model).

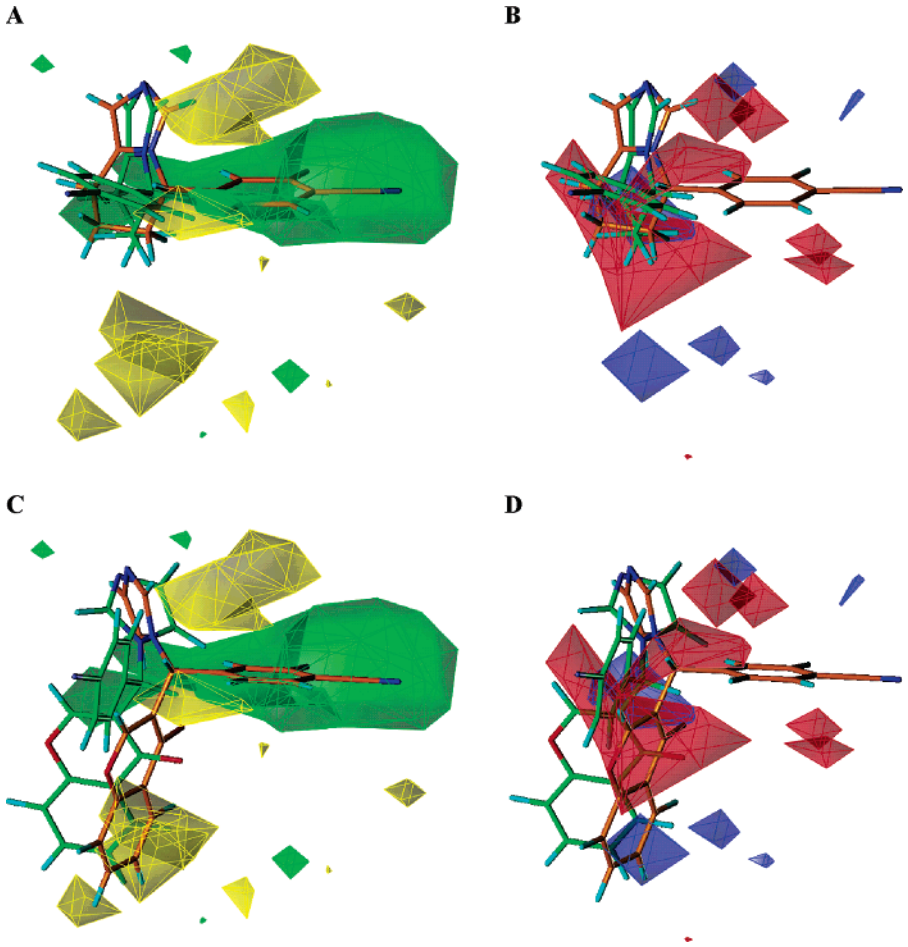

Figure 1. CoMFA contour maps plotted in the 3D space around *S*- (orange carbon atoms) and *R*-fadrozole (green carbon atoms) (A and B), and around *R*- (orange carbon atoms) and *S*-**3** (green carbon atoms) (C and D). (A and C) Steric contours: The regions where increasing the volume increases the activity are green (0.020 level), and the regions where increasing the volume decreases the activity are yellow (−0.015 level). (B and D) Electrostatic contours: The red regions indicate increase of activity with increasing positive charge (0.028 level), and the blue contours indicate increase of activity with increasing negative charge (−0.028 level).

The contour maps of the CoMFA model derived with five components (bold in Table 1) are depicted in Figure 1A,B. In agreement with our previous models,[8,9] the sterically allowed regions (green in Figure 1A) were mainly located around the *para*-CN phenyl ring of *S*-fadrozole, whereas the *para*-CN phenyl ring of *R*-fadrozole partially protruded into the sterically disallowed region (yellow in Figure 1A). In Figure 1B, the positive (red) and negative (blue) electrostatic regions are reported. While the negative CoMFA electrostatic contours were of difficult interpretation, as they split in several regions around the template skeleton, the positive (red) CoMFA contour partially surrounded the negatively charged atoms of the *para*-CN phenyl ring of *R*-fadrozole (green carbon atoms, oriented toward the reader). This result seems contradictory, but it actually means that an increase of positive charges would be required to increase the inhibitory potency in that region of the Cartesian space where the poorly active *R*-fadrozole locates its negatively charged phenyl ring.

Based on the present CoMFA model, a new series of chiral compounds was designed (**1**−**3**, Chart 2), by modifying our previously reported chromone derivatives[7] in such a way as to keep the pharmacophoric (*p*-substituted)benzylimidazole moiety and to introduce an asymmetric center on the methylene carbon atom.

The alignment strategy followed to obtain CoMFA predictions of the activity of the enantiomers of **1**−**3** was simply that of overlapping the (*p*-substituted)benzylimidazole moiety of the new compounds' enantiomers onto that of *S*- and *R*-fadrozole, respectively. This choice was made to be consistent with the alignment of all enantiomer pairs present in the training set. In Figure 1C,D, both enantiomers of **3** are shown along with the steric (Figure 1C) and electrostatic (Figure 1D) CoMFA contour maps. The *para*-CN phenyl ring of the *R* enantiomer (orange carbon atoms in Figure 1C,D) of **3** was completely embedded in the positive steric CoMFA contour (Figure 1C), whereas its *S* enantiomer (green carbon atoms in Figure 1C,D) placed the same moiety into a positive electrostatic region (Figure 1D).

The CoMFA equation was able to predict different inhibitory potencies for each enantiomer of all of the newly designed compounds, and the biological activities of the new compounds were predicted as reported in Table 2. In particular, the *R* enantiomers were always calculated more potent than the *S* ones.

After organic synthesis, enantiomer separation, configurational assignment, and biological evaluation (see below), the predicted and observed data as reported in Table 2 were compared. It turned out that the CoMFA model was able to fairly well predict the inhibitory

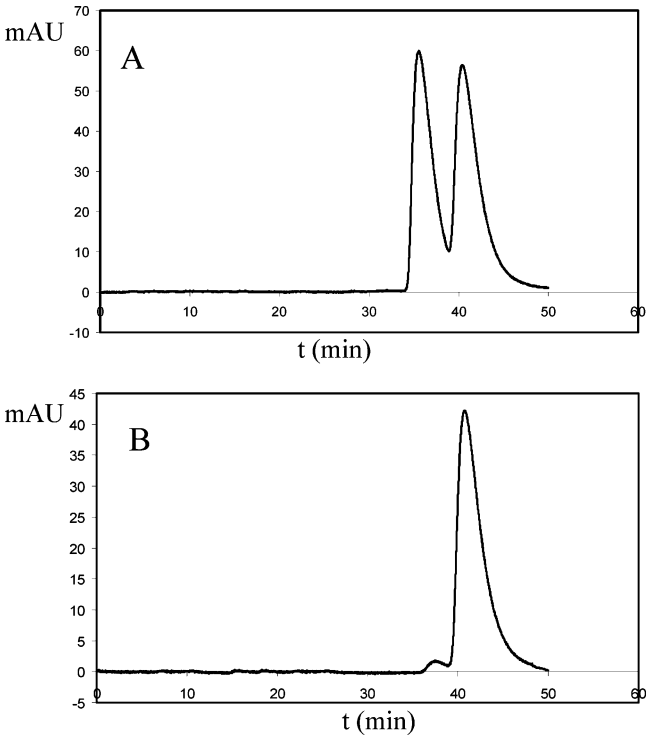

Figure 2. The enantioselective resolution of *rac*-**3** (A), upon chiralcel OD; enantiomeric excess (ee) assay of the enriched (*S*)-**3** sample (B) [r_t(first eluted enantiomer) 36.4 min; r_t(second eluted enantiomer) 40.6 min].

Table 2. Experimental and Calculated Inhibitory Activity of Molecules **1**−**3**

compd	enantiomer	pIC_{50calc}[a]	pIC_{50exp}	Δ	ΔpIC_{50exp} $(R-S)$	ΔpIC_{50calc} $(R-S)$
1	*R*	7.74	8.64	−0.90	1.62	1.59
	S	6.15	7.02	−0.87		
2	*R*	7.60	7.31	0.29	0.77	1.16
	S	6.44	6.54	−0.10		
3	*R*	7.43	6.96	0.47	0.76	1.16
	S	6.27	6.20	0.07		

[a] Calculated from the five-component model (see Table 1).

potencies of **1**−**3**. Actually, the activity of both the enantiomers of **1** was quite underpredicted (Δ = −0.90 and −0.87 for *R* and *S*, respectively). In particular, concerning *R*-**1**, this was likely due to its biological activity (pIC_{50} = 8.64), which was somewhat higher than the average activities of the 3D QSAR training set. As a matter of fact, the general limit of the CoMFA approach in predicting potencies and/or affinities of the most and least active compounds is well-known.[18,19] All of the other new derivatives were reasonably well predicted. In particular, the *S* enantiomers of **2** and **3** were predicted with errors as small as −0.10 and 0.07, respectively. More interesting, the CoMFA model was able to well predict the difference in inhibitory potency between the enantiomers of each pair. In Table 2, the ΔpIC_{50exp}-$(R-S)$ and $\Delta pIC_{50calc}(R-S)$ (i.e., the experimental and calculated differences between the biological activity of the enantiomers of **1**−**3**) are also reported. All of the predictions (1.62 vs 1.59, 0.77 vs 1.16, and 0.76 vs 1.16 for **1**, **2**, and **3**, respectively) may be considered good.

We conclude that the present CoMFA model for a series of nonsteroidal aromatase inhibitors can reasonably be considered as an example of enantioselective 3D QSAR model.

Table 3. Stereochemical Characterization of the Enantiomeric Fractions

compd	fraction	ee (%)	OR (2-propanol) at 589 nm $[\alpha]_D$	CD (2-propanol) (high energy couplet) $\Delta\epsilon$ (λ, nm)
1	less retained (*R*)	100	+46	3.1(264); −2.7(238)
	most retained (*S*)	98.2	−61	−2.7(264); 2.2(238)
2	less retained (*R*)	97.2	+54	18.2(233); −10.9(217)
	most retained (*S*)	96.2	−51	−15.3(233); 12.1(217)
3	less retained (*R*)	98.2	+94	10.3(242); −3.5(222.5)
	most retained (*S*)	96.4	−71	−9.7(242); 3.3(222.5)

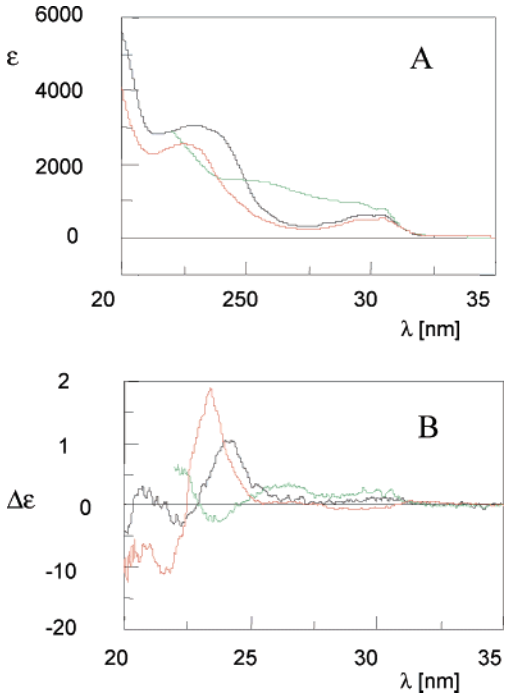

Figure 3. The UV (A) and CD (B) spectra of the first eluted enantiomers of **1** (green), **2** (red), and **3** (black) in 2-propanol solution.

Configurational Assignment. With regard to the experimental determination of chiroptical properties, Figure 2 reports the enantioselective resolution of **3** (Figure 2A), and an example of the enantiomeric excess (ee) assay of one enantiomeric fraction (Figure 2B). The ee values determined for the optically active forms of compounds **1**−**3** are reported in Table 3 along with optical rotary power (at 589 nm) and the CD data, while the absorption and CD spectra are collected in Figure 3. The availability of these chiroptical data could offer the way to assign the absolute configuration (AC) of the enantiomers of **1**−**3**. In fact, much recent progress has been made in the correct interpretation of chiroptical data by means of both coupled oscillator methods[20−27] and ab initio calculations allowing then a reliable assignment of the molecular AC: some different programs[13,28,29] for calculating ab initio the OR[30−33] at any wavelength and even the CD spectra are now available.[14,34−36] This type of approach to the AC assignment has become so powerful and reliable that it has been possible to show[37] that AC determinations carried out by X-ray diffraction analysis, considered the safest method to perform this structural determination, are incorrect and must therefore be revised. Therefore we decided to arrive at the AC of the present compounds just analyzing their chiroptical properties.

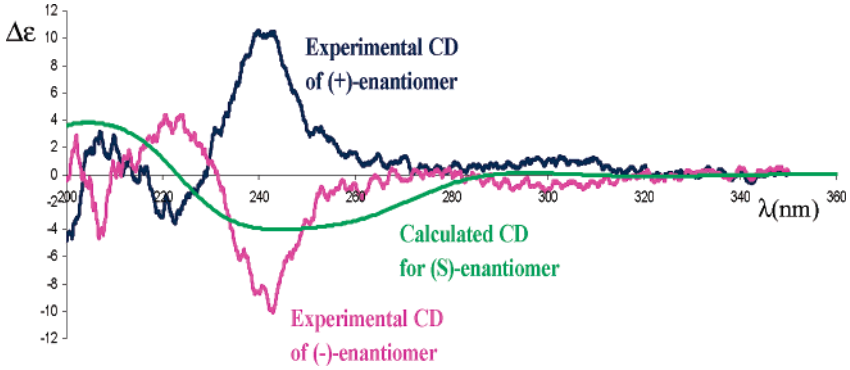

Figure 4. The weighted average CD spectrum of *S*-**3** (green) compared to the experimental CD spectra recorded for the two enantiomeric fractions in the *rac*-**3** HPLC resolution [(+)-enantiomer, less retained fraction blue; (−)-enantiomer, most retained fraction magenta].

Taking into account that intense bands are present in the absorption spectra (i.e., electronically allowed transitions occur), the analysis of the CD spectra by means of coupled oscillator techniques[20−27] after a suitable conformational analysis, and a correct assignment of the absorption bands in the electronic spectrum could be a possible strategy to provide the absolute configuration (AC). However, for the present series of compounds, some difficulties derived by the fact that, while the *para* substituted phenyl group represented a well-known chromophore, not much information is reported in the literature regarding the chromenone chromophore.[38] In addition, a further problem was represented by the location of the point-dipoles, which, in coupled oscillator treatments, represent the allowed transitions. The chromenone chromophore is not symmetric, so a decision could not be made simply on symmetry grounds. As a consequence, in order to find the correct location of point-dipoles[39−42] further calculations would have been needed.

To avoid all of these problems we decided to tackle the problem of the configurational assignment of (+)-**1**−**3** by means of the quantum mechanical methods of calculating chiroptical data: in particular we decided to start with the ab initio calculation of the optical rotation (OR) at 589 nm. To this end, OR calculations for **3** were performed, because it presents the simple symmetric CN substituent, made only by light atoms, and shows low energy Cotton effects, which determine the sign and order of magnitude of experimental OR. Thus, small basis set calculations could be confidently carried out,[43,44] significantly reducing the computational effort.

Computations at the TD-DFT level were carried out, aimed at calculating OR values to be compared to the measured ones. First, detailed conformational analyses were performed to determine the conformer populations of the compound under study. Arbitrarily, the *S* AC for **3** was assumed. A first conformational search carried out at the molecular mechanics level (MMFF94[45] of Spartan02[46]) provided 14 different conformers lying in a range of 3 kcal/mol. All of the conformations were then fully optimized at the DFT level, giving only four conformers lying in a range of 2 kcal/mol. For these conformations that were real energy minima (no imaginary frequencies), the free energy values were calculated. Actually, a more accurate evaluation of the conformer populations exploiting free energy values instead of electronic energies was pursued taking into account that, since four structures are involved in the OR calculation, the final result could be heavily affected by the conformer populations. In Figure 3SI of the Supporting Information, the 3D models of the four conformers of *S*-**3**, with their free energy and the corresponding population coming from Boltzmann statistics, are reported. In Table 2SI, the OR of each conformation along with the conformer population is reported.

The OR calculations were carried out for each conformer at the TD-DFT level and using GIAO orbitals to guarantee gauge-independency. The final result was a predicted value for *S*-**3** of −5. This number was not satisfactory, because it represented only 5% of the optical rotary power (Table 3), while only a prediction of at least 60−70% of the experimental value could reasonably constitute a reliable theoretical estimate. Therefore, to provide a safer configurational assignment, further ab initio calculations of the CD spectrum in the range 400−200 nm were carried out. In detail, the 35 lowest-energy transitions were calculated by the same TD-DFT approach. Then, the theoretical CD spectra were obtained as described in the Configurational Assignment section of the Methods.

The UV and CD spectra of the first eluted enantiomer, as obtained in 2-propanol solution, are reported in Figure 3A and 3B, respectively. Looking at the values of the OR (Table 3), it could be immediately noticed that the first eluted fraction was always dextrorotatory, suggesting that the less retained enantiomers should bear the same AC. In addition, the CD spectra of the first eluted fractions (Figure 3B) were very similar, showing a sequence of positive/negative Cotton effects between 280 and 220 nm (the positive one at about 230 nm being particularly intense). In the range 350−280 nm, only weak CD bands were present, which therefore could be considered less useful for configurational correlations. On these grounds, we could safely assume that all of the compounds were eluted with the same order, irrespective of both the *para* substitution of the phenyl ring and the used chiral stationary phase.

In Figure 4, the weighted average CD spectrum of *S*-**3** is compared to the experimental CD spectra recorded for the two enantiomeric fractions. The calculated spectrum of *S*-**3** and that of the less retained enantiomer are in a mirror image relationship. Thus, we could conclude that the AC of the less retained (+) fraction of **3** was *R*.

Table 4. Biological Activities of Compounds **1**−**3** and Fadrozole against CYP19 (Aromatase) and CYP17

compd	enantiomer	CYP19[a] IC_{50} (nM) (± se)	CYP17[b] % inhibition at 2.5 μM
1	*R*	2.3 (±1.1)	20
	S	96 (±15)	12
2	*R*	49 (±11)	17
	S	290 (±32)	13
3	*R*	110 (±28)	6
	S	630 (±55)	6
fadrozole	*S*	17 (±7)	7

[a] Substrate 1β[^{3}H]androstenedione 500 nM. [b] Substrate progesterone 25 μM.

The calculated CD spectrum did not reproduce the sign of the band at lower energy. This behavior could be due to the influence of the nature of the solvent on the related electronic transition. Indeed, the CD band of (*R*)-**3** changed sign passing from the polar 2-propanol (Figure 3) to the less polar solvent chloroform (Figure 4SI). The same behavior, i.e., inversion of the sign of the lowest energy CD band by changing the solvent polarity, was observed also in the case of compound (*R*)-**1** (Figure 3, 2-propanol; Figure 5SI, chloroform).

Biological Activity. CYP19 was prepared from human placenta.[47] The microsomes were incubated with 1β[^{3}H]androstenedione, and product formation was monitored by measuring the tritiated water formed during the aromatization of the substrate.[47] CYP17 was prepared from *E. coli* overexpressing the human enzyme.[16,17] For the inhibition test an enzyme preparation from the homogenate was incubated with progesterone. The separation of the product from the substrate was performed by HPLC.[16] The experimentally determined inhibitory potencies of **1**−**3** against aromatase are reported in Table 4 expressed as IC_{50} values. The new compounds are active at the nanomolar level, *R*-**1** being one of the most potent aromatase inhibitors so far reported ($IC_{50} = 2.3 \pm 1.1$ nM). Moreover, none of the newly synthesized compounds was significantly active toward P450 17 (Table 4), thus indicating that the set showed a good selectivity for P450 19 with respect to the androgen forming counterpart. The relative potency of *R*-**1** with respect to the marketed drug *S*-fadrozole is 7.4. This molecule is also remarkably more potent than nonsteroidal inhibitors of the azole series reported by us in the previous paper.[7] Likely, enantioselective inhibitors might fit at best the aromatase active site requirements. In this respect, it should be noted that *R*-**1**, the most potent compound of the present series, bears a NO_2 group in the *para* position of the phenyl ring, which might likely interact with a key serine residue (Ser478) of the aromatase active site, as previously suggested to be the case for the CN group of *S*-fadrozole.[48,49] However, such an argument does not help to explain the surprisingly low potency of *R*-**3**, which similarly to fadrozole bears a CN group in the *para* position of the phenyl ring. In this regard, further docking experiments using a new homology-built model will be performed in order to unravel this issue.

Conclusions

A multidisciplinary study in the field of nonsteroidal aromatase inhibitors was carried out aimed at discovering a new way to design molecules bearing enantioselectivity toward the biological counterpart. 3D QSAR studies, organic synthesis, enantiomer separation, configurational assignment, and biological assays were performed in strict collaboration to face such an important medicinal chemistry issue. In details, a new CoMFA model was obtained, adding 21 new molecules to a previously derived model. Since some of the added molecules bore a chiral atom and were enantioselective toward CYP19, the new CoMFA model was purposely exploited to design new chiral inhibitors. The 3D QSAR model predicted different activities for either enantiomer. The new molecules were synthesized and the enantiomers separated by means of preparative HPLC using a chiral stationary phase. The absolute configurational assignment was obtained by means of a combined approach based on CD measurements and TD-DFT calculations. Finally, both enantiomers of the three new derivatives were tested against human P450 19 enzyme and the experimental data were compared to the 3D QSAR equation predictions. The fairly good agreement between observed and calculated inhibition data allowed us to conclude that a properly built "enantioselective CoMFA model" might constitute a viable tool to address the design of enantioselective ligands.

Experimental Section

Computational Methods. The conformational searches were carried out using the Monte Carlo approach[50] and the MMFF94 force field[45] as implemented in the MacroModel software package.[51] In the present study, the number of Monte Carlo steps was set equal to 8000 and the trial conformation was accepted if the energy was lower than that of the previous conformation or if its energy was within an energy window of 100 kJ/mol. Then, the conformations were classified by means of a cluster analysis[52] using geometrical parameters as filtering screens. Minimum energy conformations were further optimized at the AM1 semiempirical level[53] as implemented in MOPAC. The atomic partial charges of each compound were computed by means of the RESP procedure,[12] i.e., fitting them on an electrostatic potential calculated at the DFT level. *S*-**3** was submitted to a further protocol of conformational analysis carried out by means of the SPARTAN02 suite of software at both the molecular mechanics (MMFF94 force field)[45] and semiempirical (PM3)[54] levels.

All of the ab initio quantum chemical calculations were carried out within the DFT framework using the hybrid exchange and correlation functional B3LYP[55] and the Gaussian basis set 6-31G(d). The OR calculations on the inhibitor *S*-**3** were carried out following the time dependent DFT (TD-DFT) approach and using GIAO orbitals to guarantee gauge-independency. All DFT-based calculations were performed by means of GAUSSIAN03.[13]

The 3D QSAR equations were obtained by means of the comparative molecular field analysis (CoMFA) technique.[56] The CoMFA fields were generated by using an sp^3 carbon atom with a formal charge of +1 as a probe, while the CoMFA region was generated automatically around the molecules by fixing a grid spacing of 2 Å. The statistical analyses were carried out by applying the PLS procedure to the appropriate variables and using the standard scaling method (COMFA_STD). Cross-validated PLS runs were carried out to establish the optimal number of components (the latent variables) to be used in the final fitting models. The number of cross-validated groups was always equal to the number of compounds (leave-one-out procedure), and the optimal number of components (latent variables) was chosen by considering the lowest standard error of prediction (s_{cross}). Scrambling analyses were performed to rule out the possibility of chance correlations. The CoMFA studies were carried out by means of the SYBYL software (Tripos Inc. St. Louis, MO).

Chemistry. General Methods. All melting points were determined in open glass capillaries using a Büchi apparatus and are uncorrected. ^{1}H NMR spectra were recorded on a Varian Gemini 300 spectrometer in $CDCl_3$ solutions, with Me_4-Si as the internal standard. Mass spectra were recorded on a Waters ZQ 4000 apparatus operating in electrospray (ES) mode. Elemental analyses were within 0.4% of theoretical value unless otherwise indicated. Compounds were named following IUPAC rules as applied by AUTONOM, a PC software for systematic names in organic chemistry, Beilstein-Institut and Springer.

3-(4-Nitro-benzyl)-chromen-4-one (4). A mixture of chroman-4-one (4.5 g, 0.03 mol), 4-nitrobenzaldehyde (4.6 g, 0.03 mol), and 0.4 mL of piperidine was heated at 150 °C for 3 h. After cooling, the residue was crystallized from ethyl acetate, to give 7.5 g (89.9%) of the desired compound, mp 171−172 °C. ^{1}H NMR: δ 3.85 (s, 2H), 7.35−8.25 (m, 8H, arom + H-2).

3-(4-Bromo-benzyl)-chromen-4-one (5). Using the previous procedure and starting from 4.5 g (0.03 mol) of chroman-4-one and 5.5 g (0.03 mol) of 4-bromobenzaldehyde (0.03 mol), compound **5** (7.84 g, 83%) was obtained, mp 164−167 °C. ^{1}H NMR: δ 5.30 (s, 2H), 6.90−8.15 (m, 8H, arom + H-2).

4-(4-Oxo-4*H*-chromen-3-ylmethyl)-benzonitrile (6). Using the previous procedure and starting from 4.5 g (0.03 mol) of chroman-4-one and 3.93 g (0.03 mol) of 4-cyanobenzaldehyde (0.03 mol), compound **6** (6.9 g, 88%) was obtained, mp 154−155 °C. ^{1}H NMR: δ 3.80 (s, 2H), 7.30−8.25 (m, 8H, arom + H-2).

3-[Bromo-(4-nitro-phenyl)-methyl]-chromen-4-one (7). A mixture of 3-(4-Nitro-benzyl)-chromen-4-one (**6**), (2.0 g, 0.007 mol) and *N*-bromosuccinimide (1.27 g, 0.007 mol) in the presence of a catalytic amount of benzoyl peroxide in 70 mL of CCl_4 was refluxed for 6 h and then hot filtered. The solvent was evaporated to dryness, and the residue was crystallized from ligroin, to yield 1.8 g of **7**, (64%), mp 83−85 °C. ^{1}H NMR: δ 6.45 (s, 2H), 7.40−8.35 (m, 8H, arom + H-2).

3-[Bromo-(4-bromo-phenyl)-methyl]-chromen-4-one (8). Using the previous procedure and starting from 2.25 g (0.007 mol) of **7**, compound **8** (1.92 g, 70%) was obtained, mp 136−139 °C (ligroin, lit.[57] mp 139−141 °C). ^{1}H NMR: δ 6.40 (s, 2H), 7.45−8.20 (m, 8H, arom + H-2).

4-[Bromo-(4-oxo-4*H*-chromen-3-yl)-methyl)-benzonitrile (9). Using the previous procedure and starting from 1.83 g (0.007 mol) of **8**, compound **9** (1.73 g, 73%) was obtained, mp 181−184 °C (toluene). ^{1}H NMR: δ 6.45 (s, 2H), 7.40−8.25 (m, 8H, arom + H-2).

General Method for the Preparation of the Imidazol-1-yl Derivatives (1−3). A mixture of the selected bromomethyl derivative (0.005 mol) and imidazole (0.015 mol) in 50 mL of acetonitrile was refluxed for 7 h under nitrogen. The solvent was removed under reduced pressure, and the residue was purified by flash chromatography (toluene/acetone 4:1).

3-[Imidazol-1-yl-(4-nitro-phenyl)-methyl]-chromen-4-one (1). Yield: 47%. Mp: 135−139 °C (ligroin). ^{1}H NMR ($CDCl_3$): δ 6.85 (s, 1H), 6.95−8.35 (m, 12H, arom + H-2 + CH imidazole). MS (ES): *m/z* 348 (M + H$^+$). Anal. ($C_{19}H_{13}N_3O_4$) C, H, N.

3-[(4-Bromo-phenyl)-imidazol-1-yl-methyl]-chromen-4-one (2). Yield: 52%. Mp: 133−135 °C (ligroin). ^{1}H NMR ($CDCl_3$): δ 6.80 (s, 1H), 6.95−8.20 (m, 12H, arom + H-2 + CH imidazole). MS (ES): *m/z* 381 (M + H$^+$). Anal. ($C_{19}H_{13}BrN_2O_2$) C, H, N.

4-[Imidazol-1-yl-(4-oxo-4*H*-chromen-3-yl)-methyl]-benzonitrile (3). Yield: 49%. Mp: 156−158 °C (ligroin). ^{1}H NMR ($CDCl_3$): δ 6.80 (s, 1H), 6.90−8.25 (m, 12H, arom + H-2 + CH imidazole). MS (ES): *m/z* 328 (M + H$^+$). Anal. ($C_{20}H_{13}N_3O_2$) C, H, N.

Enantioselective HPLC. The chromatographic system consisted of a Jasco PU-980 solvent delivery system, and a Jasco MD-910 multiwavelength detector connected to a computer station. A Rheodyne model 7125 injector with a 20 μL loop was used. The enantiomeric fractions of compounds **1**−**3** have been obtained by preparative HPLC resolution employing the chiral stationary phases Chiralcel OD (**1** and **3**), and Chiralcel OJ (**2**), from Daicel (Japan). Repeated injections (0.2−0.3 mg) on the 0.46 cm i.d. x 25 cm columns allowed collecting 3−6 mg of each fraction. The same columns were employed for the enantiomeric excess (ee) determination of the optically active samples. The mobile phase was a hexane/2-propanol mixture, 1 mL min^{-1}. The enantioselectivity was calculated as $\alpha = k_2/k_1$, where k_2 and k_1 are the capacity factors [k is defined as $(t_r - t_0)/t_0$; t_r = retention time of the analyte, t_0 = retention time of a nonretained solute] of the second and first eluted enantiomers, respectively.

UV, CD, and Optical Rotation Measurements. Circular dichroism and absorption spectra were carried out using a Jasco J-810 spectropolarimeter (Jasco, Tokio, Japan) and a Jasco V-530 spectrophotometer (Jasco, Tokio, Japan). All measurements were carried out in 2-propanol at room temperature, using 1−0.1 cm cells. Optical rotation measurements were carried out at 589 nm (α_D) in 2-propanol at room temperature, using an AA1000 polarimeter (Optical Activity, England), using a 10 cm cell.

Inhibitor Assays. Human placental CYP19 was prepared as described,[47] and the assay was performed according to the same reference.[47] For the CYP17 inhibition tests *E. coli* cells overexpressing human CYP17 and P450 reductase were used.[17] These cells were homogenized, and the 50.000 g sediment was employed as enzyme source.[16] The test was run as described.[16]

Acknowledgment. This work was supported by grants from MIUR-COFIN2004 (Rome, Italy). The authors thank Prof. Paolo Biscarini, (Facoltà di Chimica Industriale, Università di Bologna, Italy) for the availability of the Jasco J-810 spectropolarimeter. Financial support from Università della Basilicata to E.G. and C.R. is gratefully acknowledged.

Supporting Information Available: Elemental analysis table; structures and (experimental and calculated) aromatase inhibitory activity of the training set molecules; plot of calculated vs experimental pIC_{50} values from the CoMFA model; 3D structure and calculated OR of the low energy conformers of *S*-**3**; experimental CD spectra of *R*-**3** and *R*-**1** in chloroform. This material is available free of charge via the Internet at http://pubs.acs.org.

References

(1) Owen, C. P.; Nicholls, P. J.; Smith, H. J.; Whomsley, R. Inhibition of aromatase (P450Arom) by some 1-(benzofuran-2-ylmethyl)-imidazoles. *J. Pharm. Pharmacol.* **1999**, *51*, 427−433.
(2) Recanatini, M.; Cavalli, A.; Valenti, P. Nonsteroidal aromatase inhibitors: recent advances. *Med. Res. Rev.* **2002**, *22*, 282−304.
(3) Kim, Y. W.; Hackett, J. C.; Brueggemeier, R. W. Synthesis and aromatase inhibitory activity of novel pyridine-containing isoflavones. *J. Med. Chem.* **2004**, *47*, 4032−4040.
(4) Leonetti, F.; Favia, A.; Rao, A.; Aliano, R.; Paluszcak, A.; et al. Design, synthesis, and 3D QSAR of novel potent and selective aromatase inhibitors. *J. Med. Chem.* **2004**, *47*, 6792−6803.
(5) Woo, L. W.; Sutcliffe, O. B.; Bubert, C.; Grasso, A.; Chander, S. K.; et al. First dual aromatase-steroid sulfatase inhibitors. *J. Med. Chem.* **2003**, *46*, 3193−3196.
(6) Suzuki, T.; Moriya, T.; Ishida, T.; Kimura, M.; Ohuchi, N.; et al. In situ production of estrogens in human breast carcinoma. *Breast Cancer* **2002**, *9*, 296−302.
(7) Recanatini, M.; Bisi, A.; Cavalli, A.; Belluti, F.; Gobbi, S.; et al. A new class of nonsteroidal aromatase inhibitors: design and synthesis of chromone and xanthone derivatives and inhibition of the P450 enzymes aromatase and 17 alpha-hydroxylase/C17,-20-lyase. *J. Med. Chem.* **2001**, *44*, 672−680.
(8) Recanatini, M. Comparative molecular field analysis of non-steroidal aromatase inhibitors related to fadrozole. *J. Comput.-Aided Mol. Des.* **1996**, *10*, 74−82.
(9) Recanatini, M.; Cavalli, A. Comparative molecular field analysis of non-steroidal aromatase inhibitors: an extended model for two different structural classes. *Bioorg. Med. Chem.* **1998**, *6*, 377−388.
(10) Furet, P.; Batzl, C.; Bhatnagar, A.; Francotte, E.; Rihs, G.; et al. Aromatase inhibitors: synthesis, biological activity, and binding mode of azole-type compounds. *J. Med. Chem.* **1993**, *36*, 1393−1400.

(11) Allen, F. H. The Cambridge Structural Database: a quarter of a million crystal structures and rising. *Acta Crystallogr*. **2002**, *B58*, 380−388.
(12) Bayly, C. I.; Cieplak, P.; Cornell, W. D.; Kollman, P. A. A well-behaved electrostatic potential based method using charge restraints for determining atom-centered charges: the RESP model. *J. Phys. Chem.* **1993**, *97*, 10269−10280.
(13) Frisch, M. J.; Trucks, G. W.; Schlegel, H. B.; Scuseria, G. E.; Robb, M. A.; et al. *Gaussian 03*; Gaussian, Inc.: Pittsburgh, PA.
(14) Diedrich, C.; Grimme, S. Systematic investigation of modern quantum chemical methods to predict electronic circular dichroism spectra. *J. Phys. Chem. A* **2003**, *107*, 2524.
(15) Thompson, E. A., Jr.; Siiteri, P. K. Utilization of oxygen and reduced nicotinamide adenine dinucleotide phosphate by human placental microsomes during aromatization of androstenedione. *J. Biol. Chem.* **1974**, *249*, 5364−5372.
(16) Hutschenreuter, T. U.; Ehmer, P. B.; Hartmann, R. W. Synthesis of hydroxy derivatives of highly potent non-steroidal CYP 17 inhibitors as potential metabolites and evaluation of their activity by a non cellular assay using recombinant human enzyme. *J. Enzyme Inhib. Med. Chem.* **2004**, *19*, 17−32.
(17) Ehmer, P. B.; Bureik, M.; Bernhardt, R.; Muller, U.; Hartmann, R. W. Development of a test system for inhibitors of human aldosterone synthase (CYP11B2): screening in fission yeast and evaluation of selectivity in V79 cells. *J. Steroid Biochem. Mol. Biol.* **2002**, *81*, 173−179.
(18) Oprea, T. I.; Waller, C. L. Theoretical and Practical Aspects of Three-Dimensional Quantitative Structure−Activity Relationships. *Reviews in computational chemistry*; Indiana University-Purdue University at Indianapolis (IUPUI): Indianapolis, 1997; pp 127−182.
(19) Greco, G.; Novellino, E.; Connolly, Y. M. Approaches to Three-Dimensional Quantitative Structure−Activity Relationships. *Reviews in computational chemistry*; Indiana University-Purdue University at Indianapolis (IUPUI): Indianapolis, 1997; pp 183−240.
(20) Mason, S. F. Optical rotatory power. *Q. Rev.* **1962**, *17*, 20.
(21) Mason, S. F. *Optical rotatory dispersion and circular dichroism in organic chemistry*; Heyden and Son: London, 1967; Chapter 4, Theory II; p 71.
(22) Gottarelli, G.; Mason, S. F.; Torre, G. The circular dichroism and absolute configuration of (+)-trans-stilbene oxide. *J. Chem. Soc. B* **1971**, 1349.
(23) Harada, N.; Nakanishi, K. The exciton chirality method and its application to configurational and conformational studies of natural products. *Acc. Chem. Res.* **1972**, *5*, 257.
(24) Mason, S. F. *Molecular optical activity and the chiral discriminations*; Cambridge University Press: Cambridge, 1982.
(25) Harada, N.; Nakanishi, K. *Circular dichroic spectroscopy: exciton coupling in organic stereochemistry*; University Science Books: Mill Valley, CA, 1983.
(26) Nakanishi, K.; Berova, N. *Circular dichroism: principles and applications*; VCH Publishers Inc: New York, 1994; pp 361−398.
(27) Berova, N.; Nakanishi, K. Chapter 12. *Circular dichroism: principles and applications*, 2nd ed.; Wiley-VCH: New York, 2000.
(28) Helgaker, T.; Jensen, H. J. A.; Joergensen, P.; Olsen, J.; Ruud, K.; et al. *DALTON, a molecular electronic structure program*, 1.2 ed; University of Oslo: Oslo, Norway.
(29) Ahlrichs, R.; Bar, M.; Baron, H.-P.; Bauernschmitt, R.; Bocker, S.; et al. *TURBOMOLE*; 5.6 ed.; Universitat Karlsruhe: Karlsruhe, Germany.
(30) Polavarapu, P. L. Ab initio molecular optical rotations and absolute configurations. *Mol. Phys.* **1997**, *91*, 551.
(31) Kondru, R. K.; Wipf, P.; Beratan, D. N. Theory-assisted determination of absolute stereochemistry for complex natural products via computation of molar rotation angles. *J. Am. Chem. Soc.* **1998**, *120*, 2204.
(32) Stephens, P. J.; Devlin, F. J.; Cheeseman, J. R.; Frisch, M. J. Calculation of optical rotation using Density Functional Theory. *J. Phys. Chem. A* **2001**, *105*, 5356.
(33) Polavarapu, P. L. Optical rotation: recent advances in determining the absolute configuration. *Chirality* **2002**, *14*, 768.
(34) Pedersen, T. B.; Koch, H. Theoretical electronic absorption and natural circular dichroism spectra of (−)-trans-cyclooctene. *J. Chem. Phys.* **2000**, *112*, 2139.
(35) Furche, F.; Ahlrichs, R.; Wachsmann, C.; Weber, E.; Sobanski, A.; et al. Circular dichroism of helicenes investigated by time-dependent Density Functional Theory. *J. Am. Chem. Soc.* **2000**, *122*, 1717.
(36) Braun, M.; Hohmann, A.; Rahematpura, J.; Buehne, C.; Grimme, S. Synthesis and determination of the absolute configuration of fugomycin and desoxyfugomycin: CD spectroscopy and fungicidal activity of butenolides. *Chem.—Eur. J.* **2004**, *10*, 4584.
(37) Devlin, F. J.; Stephens, P. J.; Besse, P. Are the absolute configurations of 2-(1-hydroxyethyl)-chromen-4-one and its 6-bromo derivative determined by X-ray christallography correct? A vibrational circular dichroism study of their acetate derivatives. *Tetrahedron: Asymmetry* **2005**, *16*, 1557−1566.
(38) Harada, N.; Ono, H.; Uda, H.; Parveen, M.; Khan, N.; et al. Atropisomerism in natural products. Absolute stereochemistry of biflavone, (−)-4′,4‴,7,7″-tetra-O-methylcupressuflavone, as determined by the theoretical calculation of CD spectra. *J. Am. Chem. Soc.* **1992**, *114*, 7687.
(39) Mason, S. F. Non-anomalous absolute configuration of 1,5-disubstituted-9,10dihydro-9,10-bridged anthracenes. *J. Chem. Soc., Chem. Commun.* **1973**, 239.
(40) Gottarelli, G.; Proni, G.; Spada, G. P.; Fabbri, D.; Gladiali, S.; et al. Conformational and configurational analysis of 4,4′-biphenanthryl derivatives and related helicenes by circular dichroism spectroscopy and cholesteric induction in nematic mesophases. *J. Org. Chem.* **1996**, *21*, 2013.
(41) Tanaka, K.; Pescitelli, G.; Di Bari, L.; Xiao, T. L.; Nakanishi, K.; et al. Absolute stereochemistry of dihydrofuroangelicins bearing C-8 substituted double bonds: a combined chemical/exciton chirality protocol. *Org. Biomol. Chem.* **2004**, *2*, 48.
(42) Giorgio, E.; Maddau, L.; Spanu, E.; Evidente, A.; Rosini, C. Assignment of the Absolute Configuration of (+)-Diplopyrone, the Main Phytotoxin Produced by Diplodia mutila, the Pathogen of the Cork Oak Decline, by a Nonempirical Analysis of its chiroptical properties. *J. Org. Chem.* **2005**, *70*, 7.
(43) Giorgio, E.; Minichino, C.; Viglione, R. G.; Zanasi, R.; Rosini, C. Assignment of the molecular absolute configuration through the ab initio Hartree−Fock calculation of the optical rotation: can the circular dichroism data help in reducing basis set requirements? *J. Org. Chem.* **2003**, *68*, 5186.
(44) Giorgio, E.; Viglione, R. G.; Rosini, C. Assignment of the absolute configuration of large molecules by ab initio calculation of the rotatory power within a small basis set scheme: the case of some biologically active natural products. *Tetrahedron: Asymmetry* **2004**, *15*, 1979.
(45) Halgren, T. A. Merck molecular force field. I. Basis, form, scope, parameterization, and performance of MMFF94. *J. Comput. Chem.* **1996**, *17*, 490−519.
(46) *SPARTAN '02*; Wavefunction Inc.: Irvine, CA.
(47) Hartmann, R. W.; Batzl, C. Aromatase inhibitors. Synthesis and evaluation of mammary tumor inhibiting activity of 3-alkylated 3-(4-aminophenyl)piperidine-2,6-diones. *J. Med. Chem.* **1986**, *29*, 1362−1369.
(48) Cavalli, A.; Greco, G.; Novellino, E.; Recanatini, M. Linking CoMFA and protein homology models of enzyme−inhibitor interactions: an application to non-steroidal aromatase inhibitors. *Bioorg. Med. Chem.* **2000**, *8*, 2771−2780.
(49) Cavalli, A.; Recanatini, M. Looking for selectivity among cytochrome P450s inhibitors. *J. Med. Chem.* **2002**, *45*, 251−254.
(50) Chang, G.; Guida, W. C.; Still, W. C. An internal coordinate Monte Carlo method for searching conformational space. *J. Am. Chem. Soc.* **1989**, *111*, 4379−4386.
(51) Mohamadi, F.; Richards, N. G. J.; Guida, W. C.; Liskamp, R. M. J.; Lipton, M. A.; et al. MacroModel—an integrated software system for modeling organic and bioorganic molecules using molecular mechanics. *J. Comput. Chem.* **1990**, *1*, 440−467.
(52) Shenkin, P. S.; McDonald, D. Q. Cluster analysis of molecular conformations. *J. Comput. Chem.* **1994**, *15*, 899−916.
(53) Dewar, M. J. S.; Zoebisch, E. G.; Healy, E. F.; Stewart, J. P. P. AM1: a new general purpose quantum mechanical molecular model. *J. Am. Chem. Soc.* **1985**, *107*, 3902−3909.
(54) Stewart, J. P. P. Optimization of parameters for semiempirical methods I. Method. *J. Comput. Chem.* **1989**, *10*, 209−220.
(55) Becke, A. D. A new mixing of Hartree−Fock and local density-functional theories. *J. Chem. Phys.* **1993**, *98*, 1372−1377.
(56) Cramer, R. D. r.; Patterson, D. E.; Bunce, J. D. Comparative molecular field analysis (CoMFA). 1. Effect of shape on binding of steroids to carrier proteins. *J. Am. Chem. Soc.* **1988**, *110*, 5959−5967.
(57) Patonay, T.; Dinya, Z.; Lèvai, A.; Molnar, D. Reactivity of a-arilidene benzoheteracyclanone dibromides toward azide ion: an effective approach to 3-(substituted-benzyl chromones and 1-thiochromones. *Tetrahedron* **2001**, *57*, 2895−2907.

JM058042R